Zero-Point Tunneling Splittings in Compounds with Multiple Hydrogen Bonds Calculated by the Rainbow Instanton Method

ARTICLE *in* THE JOURNAL OF PHYSICAL CHEMISTRY A · OCTOBER 2013

Impact Factor: 2.69 · DOI: 10.1021/jp4073608 · Source: PubMed

3 AUTHORS, INCLUDING:

Willem Siebrand
National Research Council Canada
202 PUBLICATIONS **5,615** CITATIONS

SEE PROFILE

Antonio Fernández-Ramos
University of Santiago de Compostela
84 PUBLICATIONS **1,832** CITATIONS

SEE PROFILE

THE JOURNAL OF PHYSICAL CHEMISTRY A

Article

pubs.acs.org/JPCA

Zero-Point Tunneling Splittings in Compounds with Multiple Hydrogen Bonds Calculated by the Rainbow Instanton Method

Zorka Smedarchina,*[,†] Willem Siebrand,[†] and Antonio Fernández-Ramos[‡]

[†]National Research Council of Canada, 100 Sussex Drive, Ottawa, K1A 0R6 Canada

[‡]Department of Physical Chemistry and Center for Research in Biological Chemistry and Molecular Materials (CIQUS), University of Santiago de Compostela, 15706 Santiago de Compostela, Santiago de Compostela, Spain

ABSTRACT: Zero-point tunneling splittings are calculated, and the values are compared with the experimentally observed values for four compounds in which the splittings are due to multiple-proton transfer along hydrogen bonds. These compounds are three binary complexes, namely, the formic acid and benzoic acid dimer and the 2-pyridone-2-hydroxypyridine complex, in which the protons move in pairs, and the calix[4]arene molecule, in which they move as a quartet. The calculations make use of and provide a test for the newly developed rainbow approximation for the zero-temperature instanton action which governs the tunneling splitting (as well as the transfer rate). This approximation proved to be much less drastic than the conventional adiabatic and sudden approximations, leading to a new general approach to approximate the instanton action directly. As input parameters the method requires standard electronic-structure data and the Hessians of the molecule or complex at the stationary configurations only; the same parameters also yield isotope effects. Compared to our earlier approximate instanton method, the rainbow approximation offers an improved treatment of the coupling of the tunneling mode to the other vibrations. Contrary to the conventional instanton approach based on explicit evaluation of the instanton trajectory, both methods bypass this laborious procedure, which renders them very efficient and capable of handling systems that thus far have not been handled by other theoretical methods. Past results for model systems have shown that the method should be valid for a wide range of couplings. The present results for real compounds show that it gives a satisfactory account of tunneling splittings and isotope effects in systems with strong coupling that enhances tunneling, thus demonstrating its applicability to low-temperature proton dynamics in systems with multiple hydrogen bonds.

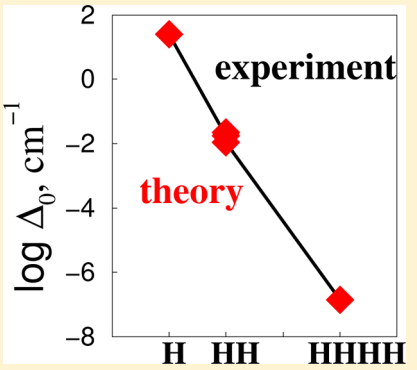

1. INTRODUCTION

In systems containing more than one hydrogen bond, multiple-proton transfer along these bonds may occur. Transfer of this type can be detected as tunneling splitting in isolated compounds or as a reaction rate in compounds embedded in a medium. It has been observed in a variety of compounds of chemical and biological interest, ranging from carboxylic acid dimers to DNA.[1,2] Depending on the conditions, transfer may be stepwise or concerted, but at very low temperatures only concerted transfer will survive. Thus to calculate, for example, zero-point tunneling splittings, corresponding to coherent tunneling at zero temperature ($T = 0$), we can focus on concerted transfer across a single barrier. Nevertheless this process will be more complex than single-proton transfer since the vibrational pattern will be more complicated. In single-proton transfer, the tunneling motion is coupled predominantly to a single skeletal mode, the vibration of the hydrogen bridge, but in multiple-proton transfer, there will be two or more of these bridge vibrations which will generally be coupled, creating a pattern that complicates the calculations. Although biological interest in these processes is mainly focused on the rates of reaction, to test a theoretical method, the investigation of tunneling splittings has the advantage of allowing calculations to be made of isolated molecules or complexes suitable for spectroscopic investigation, thus holding promise for clear and unambigious results. Hence such investigations are very useful to test theoretical approaches to proton transfer. Because of the large number of degrees of freedom involved, direct-diagonalization approaches to the molecular Hamiltonian to the level of accuracy required to account for small splittings become unwieldy for all but the smallest systems. As discussed below, specialized methods have been developed to deal with this problem, including some in which the proton tunneling causing the splitting is treated as a dynamic phenomenon, but practical applications to multiple-proton transfer are few. The only system of this kind for which high-resolution spectra as well as several high-level calculations are available is the formic acid dimer (FAD), the simplest dimeric carboxylic acid. The zero-point splitting in this molecule and a dideutero isotopomer, with the deuterium attached to carbon rather than oxygen, has been measured accurately by Havenith et al.,[3,4] who, however, found the earlier calculations[5−9] to be unhelpful when they encountered an ambiguity in the assignment of the spectra of the isotopomer.[3] They observed

Received: July 24, 2013
Revised: September 26, 2013

   dx.doi.org/10.1021/jp4073608 | J. Phys. Chem. A XXXX, XXX, XXX−XXX

two splittings differing by a factor close to 4 and tentatively assigned the smaller splitting to the zero-point level and the larger one to an excited CO-stretch level. Subsequent calculations aimed at firming up this assignment remained ambiguous,[10−12] until our work[13,14] based on the approximate instanton method (AIM)[15,16] succeeded in calculating the splittings of both levels, which allowed us to reverse the assignment, a reversal that was subsequently confirmed by measurements on the parent compound.[4]

There are only a few other compounds involved in concerted multiple-proton transfer for which both observed and calculated zero-point splittings have been reported. For the benzoic acid dimer[14,17] (BAD) and the 2-pyridone-2-hydroxypyridine complex[18−20] (2PH-2PY), splittings are reported as the sums and differences of the splitting of the zero-point levels of the ground state and the first singlet excited state, but for both complexes the original authors have argued cogently that the dominant contribution should be that of the ground state, since the electronic excitation is effectively localized on one of the two components of the complex, which obstructs exchange.[17,20] For both complexes, we have reported calculations based on the AIM as implemented in the DOIT code.[16] As the earlier reports[14,19] show, the results have been relatively good, but the procedure has been complicated by a problem that is typical for hydrogen bonds, namely, the strong coupling between the tunneling vibration and the symmetric skeletal mode(s) of the hydrogen bond bridge(s). The AIM is based on an approach in which one-dimensional (1D) tunneling is corrected for such couplings by first grouping the modes into "fast" and "slow" modes relative to the imaginary frequency under the barrier and then using the adiabatic and sudden approximations, respectively, to calculate the couplings, treated as additive, within each group. However, this grouping is not always unambiguous. Especially in the case of hydrogen bonds, the frequency of the most strongly coupled modes tends to be comparable to the tunneling frequency, so that the assignment as fast or slow is not automatically controlled by the code and must be made on physical grounds, which may not always be evident.

To overcome this handicap, we recently[21] introduced the rainbow instanton method (RIM), which is based on essentially the same approximate Hamiltonian used with the AIM, but treats the coupling between the tunneling motion and the remaining coordinates in a different way. Tunneling splittings in compounds with 2-fold symmetry can be described in terms of a multidimensional (MD) potential energy surface (PES) with two equivalent minima separated by a symmetric barrier. In the instanton approach the overall tunneling probability is expressed as a sum over all paths $s(t)$ connecting the minima (a path integral), each contributing with the phase factor $\exp(iS)$, where S is the classical action (hereafter action is in units $\hbar$). The resulting oscillatory behavior is overcome by transformation to imaginary time $t \rightarrow t' = it$, each path acquiring the "weight" $\exp(-S_E)$, where $S_E = \int dt'\ H[s(t')]$ is the Euclidean action, defined via the Hamiltonian $H = 1/2\dot{s}^2 + V(s)$, instead of the Lagrangean; it describes classical motion in the upside-down potential $V(s) \rightarrow -V(s)$. The integral is dominated by the instanton path, denoted by s_I, in which the tunneling probability reaches its maximum value, defined by the equation for the extremum $\delta S_E = 0$. The tunneling probability is then defined by a single term: $P \approx \exp(-S_I)$, where $S_I = \int dt'[1/2\ \dot{s}_I^2 + V(s_I)]$ is the action evaluated along the extreme path, hereafter called instanton action. Specifically, the zero-point tunneling splitting (and the low-temperature tunneling rate) is defined by the instanton action evaluated at $T = 0$. The traditional approach, pursued by Tautermann,[22] Meana-Pañeda et al.,[23] Mil'nikov and Nakamura,[24] and, more recently, by Althorpe[25,26] and by Rommel and Kästner,[27] involves a search for the instanton trajectory via the direct minimization of the Euclidean action, and then evaluating that action along this path. Thus the MD potential (and the action) is generated on a grid in the configuration space of $3N - 6$ dimensions, N being the number of atoms, until the trajectory is found in which the action reaches its minimal value. This approach requires, on the one hand, a sufficiently dense grid, and on the other, an accurate evaluation of the MD potential in each point. In application to systems of practical interest of the type studied here, its cost may be prohibitive unless simplifications are introduced in the description of the potential or the density of the grid. Also, since the instanton path is not the same for different isotopomers, extension to, for example, deuterium tunneling requires a repeat of the entire calculation.

We adopt an alternative approach that allowed us to approximate the instanton action directly, without explicit search of the instanton path; the results on the FAD, mentioned above and discussed in more detail in section 5.2, suggest that the corresponding loss of accuracy compares favorably with that resulting from the simplifications required to keep the method discussed in the preceding paragraph tractable. Our approach takes advantage of the symmetry of the system with respect to reflection in the dividing plane, defined as $x = 0$, and recognizes that the instanton must coincide with the direction x perpendicular to it in the vicinity of this plane. Therefore a (symmetric) double-minimum potential $V(x)$ that connects the minima is already a good zero-order approximation, but since x does not coincide with the instanton throughout, coupling terms are needed for the remaining $3N - 7$ degrees of freedom $\{y\}$ perpendicular to x. As a coordinate set we choose the normal modes $(x,\{y\})$ of the transition state (TS) configuration, which is the configuration of highest symmetry, and adopt the mode x with imaginary frequency as the "reaction coordinate". This choice allows the direct generation of the MD potential in the form of $V(x) + \omega_i^2 y_i^2/2 + c_s x^2 y + c_a x y_a$, where the lowest-order coupling terms allowed by symmetry are linear in $\{y\}$, which are treated as harmonic oscillators. Only modes that are displaced between the stationary configurations contribute to this coupling, namely, modes that are symmetric/antisymmetric with respect to reflection in the dividing plane, indicated by subscripts s/a, respectively, here used as collective labels. The corresponding coupling constants $c_{s,a}$ are proportional to the displacements of the modes. Higher-order coupling terms are not explicitly included in the treatment, but are indirectly accounted for through the rescaling of the constants c_i. Such couplings are not only intrinsically smaller than the linear couplings, but can also be of either sign and thus are subject to mutual cancellation. Obviously, the reduction in dimensionality by the elimination of all modes that are not significantly displaced implies a drastic simplification of the problem.

The 1D double-minimum potential used in the RIM is in fact the adiabatic potential $V_{ad}(x)$, that is, a potential with all the coupled modes relaxed; it is taken in the form of an analytical function of the quartic type, found adequate for proton-transfer along hydrogen bonds. The MD potential in this approximation and the corresponding Hamiltonian are thus generated from standard electronic-structure data and the Hessians for the two

dx.doi.org/10.1021/jp4073608 | J. Phys. Chem. A XXXX, XXX, XXX−XXX

stationary configurations only, namely, the equilibrium configuration (EQ) and the TS; this "imaginary-mode" Hamiltonian is essentially the same as that employed in the AIM and was first introduced as early as 1995 (see ref 21, in which the RIM was introduced, and the original papers cited therein). To solve the instanton problem for this Hamiltonian, we take advantage of the fact that the equations $\delta S_E/\delta x = 0$ and $\delta S_E/\delta y_i = 0$, which define the extreme trajectory, can be solved exactly for the harmonic modes $\{y\}$, which yields a quasi-1D instanton problem for the reaction coordinate only. The Euclidean action for this problem consists of a "local" term, corresponding to 1D motion in $V_{ad}(x)$, and a "nonlocal" term of the time-retarded interaction, which reflects the "memory" of the coupled oscillators and is governed by exponential kernels. If the oscillators are fast or slow relative to the tunneling motion, these kernels can be treated approximately, leading to the well-known "slow-flip" or "fast-flip" instanton solutions, respectively. The resulting picture is again that of a 1D tunneling along the reaction coordinate, but with renormalized potential and mass; these approximations, known also as the adiabatic or sudden approximation, respectively, are the basis of the AIM. If the oscillators are neither fast nor slow on the tunneling timescale, the memory effects need to be treated explicitly. The main idea of the RIM is in the recognition that, independent of the coupled-mode frequency, the nonlocal term is relatively small and therefore needs to be evaluated only approximately; this holds for the whole range of coupling strength: at weak coupling because the coefficients corresponding to the individual modes are small, and at strong coupling because the memory kernels fall off rapidly. This leads to a new general approach to approximate the instanton action directly, whereby the memory kernels are kept intact, but an approximate instanton solution is used instead.

The new approximation proved to be much less drastic than the conventional adiabatic and sudden approximations; it can handle a wide range of vibrational frequencies that bridge the gap between the limits in which these approximations apply and was therefore termed the rainbow approximation. The method yields a readily evaluated expression for the zero-temperature instanton action applicable to any system. This was shown in the tests of 2D systems in ref 21, in which excellent agreement with the exact instanton results was obtained for the whole range of parameters involved. Another advantage of the new approach over the AIM is that any ambiguity in assigning a mode to the "fast" or the "slow" group affects only the (small) nonlocal action and leaves the main adiabatic action untouched.

The new method, developed so far for zero-point splitting, was applied successfully to the single-proton transfer in malonaldehyde (MA).[21] Here we apply it to the three complexes listed above, which will be a sterner test, as well as to the data recently reported for quadruple-proton transfer in calix[4]arene[28] (CLX), in which the proton transfer rate rather than the tunneling splitting was deduced from the measurements. Our continuing aim is to develop an efficient method to calculate tunneling splittings and proton transfer rates in polyatomics, in which protons often move in pairs. We offer the calculations reported here, which include predictions as well as comparisons with our earlier calculations, as a first indication of the capability of the RIM in this field. All the results have been obtained with a code available to interested readers.[29]

2. THE IMAGINARY-MODE HAMILTONIAN

The Hamiltonion used in our instanton calculations has been discussed several times,[15,21,30] but since it has recently been successfully extended to deal with excited-level splittings,[31] we repeat its main features. We consider a molecule (complex, radical, etc.) with two equivalent EQ configurations separated by a symmetric potential-energy barrier that allows passage of a light particle, for example, a proton, by quantum-mechanical tunneling, thereby converting one EQ into the other. The top of the barrier thus acts as a TS; as the point of highest symmetry, it serves as the origin of the vibrational coordinates. To determine these coordinates, we solve the Schrödinger equation for TS and the corresponding Hessian. This yields a set of (mass-weighted) coordinates x,y_i with harmonic (boldfaced, i.e. dimensioned) frequencies $\boldsymbol{\omega}^*$ and $\boldsymbol{\omega}_i$, where $\boldsymbol{\omega}^*$ is the imaginary frequency along the "reaction coordinate" x.

To be able to use these same coordinates for the entire region between the TS and the EQ, we solve the Schrödinger equation for the EQ, calculate the corresponding Hessian, and then introduce a number of assumptions that allow us to represent the changes that occur along the coordinates y_i by coupling terms of the form xy_i and x^2y_i. The need for coupling terms proportional to both x and x^2 follows from symmetry considerations; the modes y_i that are antisymmetric with respect to reflection in the dividing plane, denoted by i = a, have the same symmetry as the tunneling mode and thus contribute coupling terms xy_a, while the symmetric modes i = s contribute coupling terms x^2y_s. The assumptions lead to a PES in the form of a double-minimum potential along x that connects the minima and coupling terms to the modes i = a,s that are treated as harmonic oscillators. By definition, the kinetic energy operator is diagonal in the most important region close to the barrier top; it is taken to be diagonal throughout. The MD Hamiltonian then takes the general form:

$$H = \frac{1}{2}\dot{x}^2 + \frac{1}{2}\sum_i \dot{y}_i^2 + V_{1D}(x) + \frac{1}{2}\sum_i \boldsymbol{\omega}_i^2 y_i^2 - x^2\sum_{i=s} c_i y_i - x\sum_{i=a} c_i y_i \quad (1)$$

In our approach $V_{1D}(x)$ is the 1D "crude-adiabatic" potential along the reaction coordinate, evaluated with modes y_i fixed in their equilibrium configurations $y_{i=s} = \Delta y_{i=s}$ and $y_{i=a} = \pm\Delta y_{i=a}$; it is analogous to the potential along the linear reaction path. In the rainbow approach, the dynamics along the reaction coordinate is in fact governed not by $V_{1D}(x)$ but by the adiabatic potential $V_{ad}(x)$, that is, the potential evaluated with the modes y_i relaxed. The height and width of this potential are calculated parameters. For the instanton calculations, one needs the shape of this potential between the EQ and the TS; we approximate it by a quartic function, which was found adequate in our earlier studies. The coupling parameters c_i in eq 1 are given by

$$c_{i=a} = \boldsymbol{\omega}_i^2 \Delta y_i/\Delta x; \qquad c_{i=s} = \boldsymbol{\omega}_i^2 \Delta y_i/\Delta x^2 \quad (2)$$

where Δx is the half-width of the barrier. The MD Hamiltonian, shown in eq 1, in this order of approximation can be generated from standard electronic-structure data and the Hessians for the stationary configurations only; details are given in the Appendix and ref 21.

The coupling terms that are proportional to y_i can only represent the displacement of the modes between the TS and

dx.doi.org/10.1021/jp4073608 | J. Phys. Chem. A XXXX, XXX, XXX–XXX

the EQ; this restriction to linearity, imposed by the instanton formalism in our approach, as shown below, means that frequency changes are neglected. However, for the frequency of the tunneling mode in the EQ we use the calculated value. In the RIM we go one step further by recalibrating the coupling parameters c_i to reproduce the calculated adiabatic barrier height; this amounts to including some of the quadratic and higher-order couplings; the effect of these terms turns out to be small for zero-point splittings because these terms can be of either sign, leading to effective cancellation. (For a more extensive discussion of the Hamiltonian, see ref 21). However, we note that for excited-level splitting it is necessary to add the cross terms between modes that interchange during the tunneling event. With this addition, the Hamiltonian accounted qualitatively for *all* the 17 observed excited-level splittings in MA,[31] about half of which were predicted, that is, proposed before the observed values were reported.[32] These results, which do not involve instanton calculations, provide a test for the validity of the imaginary-mode Hamiltonian.

3. THE RAINBOW APPROACH TO ZERO-POINT TUNNELING SPLITTING

This section lists the basic equations of the rainbow approximation required to calculate the tunneling splittings in the compounds under discussion. A summary of the approach is presented in the Appendix; complete derivations can be found in ref 21. As introduced above, the zero-point tunneling splitting is defined by the Euclidean action S_I evaluated along the "instanton trajectory" at $T = 0$:

$$\Delta E_0 = \mathcal{A} \exp(-S_I) \tag{3}$$

The pre-exponent $\mathcal{A}$ reflects the fluctuations about the instanton trajectory and is of the general form $\mathcal{A} = \Gamma(2S_I/\pi)^{1/2}$, where Γ depends on the specific form of the potential along this trajectory. Since in our approach the main part of S_I is defined by the adiabatic potential, which in the applications takes the form of a quartic function, as specified below, we use the known approximate expression for such a potential, namely,

$$\mathcal{A} = (\hbar\boldsymbol{\omega}_0/\pi)\sqrt{24\pi S_I} \tag{4}$$

where $\boldsymbol{\omega}_0$ is the harmonic frequency of the tunneling mode in the EQ.

The main parameter to be evaluated is thus the instanton action S_I, which we evaluate with the RIM based on the MD Hamiltonian specified in section 2. As detailed in the Appendix, the application of standard instanton techniques to this Hamiltonian leads to an effective 1D instanton problem for the reaction coordinate. The corresponding Euclidean action consists of a local term, a single-time integral, and a nonlocal term, a double-time integral that is difficult to evaluate. The local term, which dominates, is represented by the 1D Hamiltonian of motion in the adiabatic potential $V_{ad}(x)$. The nonlocal term, which is positive and smaller but not negligible, represents the time-retarded interaction and is governed by exponential kernels. In the rainbow approach, this term is treated in a new way, whereby no approximations are applied to the kernels, but an approximate instanton solution is used instead. This yields the following expression for the instanton action in eqs 3 and 4:

$$S_I = (V_0/\hbar\Omega)[C_a\tilde{S}_{I,s} + \Delta S_a];$$
$$\tilde{S}_{I,s} = \tilde{S}_{ad} + \tilde{S}^0_{nl,s}; \quad \tilde{S}_{ad} = (4/3)\sqrt{2(1 - \tilde{B}_s)} \tag{5}$$

where V_0 is the barrier height along the crude-adiabatic potential and Ω is the "scaling frequency" defined by the barrier height and half-width as $\Omega^2\Delta x^2 = V_0$; V_0 and Δx are both calculated parameters (hereafter we use ordinary symbols for dimensionless frequencies scaled by Ω to distinguish them from the dimensioned frequencies, which are in bold symbols). The quantities C_a and ΔS_a in eq 5 are correction terms that are needed because of the coupled (antisymmetric) a-modes, namely, the mass-renormalization due to "fast" modes and the familiar Franck−Condon factor $\exp(-2\Delta S_a)$ due to "slow" modes. They are small for the hydrogen-bond systems under consideration ($C_a \approx 1$, $\Delta S_a < 1$); details can be found in ref 21. The tildes indicate that the parameters of the remaining (symmetric) s-modes are rescaled to include the effect of the (weak) antisymmetric coupling; specifically, $\tilde{B}_s$ is the total coupling constant of the s-modes, defined in eq A.6, with small corrections for the a-modes. Although all these corrections are duly included in the applications presented below, they add no new insight and need not concern us here. We thus focus on the evaluation of the two major contributions to the instanton action $\tilde{S}_{I,s}$ defined by the strong symmetric coupling: the adiabatic term $\tilde{S}_{ad}$, which dominates, and the nonlocal term $\tilde{S}^0_{nl,s}$, which provides a modest but nonnegligible correction; the superscript 0 indicates that it is obtained with an approximate instanton solution $Q^0(\tau)$ ($Q = x/\Delta x$ is the dimensionless reaction coordinate scaled by the barrier half-width).

The former term represents the instanton action of 1D motion in the adiabatic potential $V_{ad}(x)$ along the reaction coordinate; for its evaluation we need to generate this potential between the stationary points $x = 0$ and $x = \Delta x$, as required in the instanton formalism. From the electronic-structure data and the Hessians at the TS and the EQ we know its barrier height $V_{ad}(0)$ and half-width Δx, as well as its respective curvatures $|\boldsymbol{\omega}^*|$ and $\boldsymbol{\omega}_0$; it should interpolate smoothly in the intermediate range. As mentioned above, for proton-transfer processes such interpolations are well approximated by an analytical function of the quartic type. This approximation has been tested several times in the past in comparison with actual numerical potentials evaluated point-by-point along the minimal energy path and was found to be satisfactory for hydrogen bonds.[16,30] The height $V_{ad}(0)$ of the adiabatic potential, which is the most important parameter of any tunneling approach, is related to V_0 by $V_{ad}(0) = (1 - B)V_0$, where B, the main coupling parameter, obtained from the displacements of the coupled modes between the TS and the EQ, is approximated here by $\tilde{B}_s$, as indicated above. All the results presented here are derived for the adiabatic potential in the quartic form specified in eq A.5. We note, however, that the rainbow method is not limited to the quartic potential; we use it here because it has the advantage of allowing analytical solutions that make the treatment more transparent.

The nonlocal term in question is related to the symmetric modes and forms the nucleus of the problem addressed in ref 21. It deals with couplings of the tunneling to modes that operate on the same time scale, that is, to those modes in which frequency is comparable to the magnitude $|\boldsymbol{\omega}^*|$ of the imaginary frequency of the TS. The characteristic time of tunneling in the adiabatic potential is the reciprocal of $|\boldsymbol{\omega}^*|$ so that, in dimensionless units $\tau = \Omega t$, it is given by $\tau^* = 1/(1 - B)^{1/2}$.

dx.doi.org/10.1021/jp4073608 | J. Phys. Chem. A XXXX, XXX, XXX−XXX

Table 1. The Effect[a] of Strong Symmetric Coupling on Proton Tunneling in Malonaldehyde (MA) Treated in ref 21; the Formic Acid Dimer (FAD); the Benzoic Acid Dimer (BAD); the 2-Pyridone-2-hydroxypyridine (2PH-2PY) Complex, and Calixarene (CLX) and Input Parameters for the Rainbow Calculations Derived from Standard Quantum-Chemical Data[b]

compound	$V_{ad}(0)$	V_0	R_{EQ}/R_{TS}	Δx	ω_0	Ω	B_s	B_a
MA[c]	4.08	14.44	2.62/2.36	0.430	2642	960	0.70	0.02
FAD[d]	7.93	27.60	2.70/2.40	0.585	2946	975	0.66	0.05
BAD[e]	7.33	21.43	2.69/2.42	0.585	2749	859	0.57	0.09
2PH-2PY[f]	8.35	24.26	2.64/2.40	0.596	2759	897	0.61	0.04
			2.91/2.58					
CLX[g]	19.97	49.60	2.67/2.40	0.742	3009	1031	0.57	0.03

[a]The first three columns list the heights (in kcal/mol) of the adiabatic barrier, $V_{ad}(0)$, and the crude adiabatic barrier, V_0, along the reaction coordinate, and the shortening of the hydrogen bridge length R_{TS} in the transition state relative to the equilibrium configuration R_{EQ} (in Å). [b]Namely, the mass-weighted half-width Δx of the adiabatic barrier (in Å amu$^{1/2}$); the frequency along the reaction coordinate in the well ω_0 and the scaling frequency Ω (in cm^{-1}); and the (dimensionless) contributions $B_{s,a}$ of symmetric and antisymmetric modes, respectively, to the main coupling parameter B. Note that $V_{ad}(0) = (1 - B)V_0$. The ratio $V_0/(\hbar\Omega)$ is the scaling coefficient in eq 5. The distances R_{EQ}/R_{TS} on lines 4 and 5 refer to the O−O and N−N bridges, respectively. [c]Reference 21. [d]Reference 13. [e]Reference 14. [f]Reference 20. [g]This work.

This allows us to divide the coupled modes ω_i into "fast" and "slow" modes according to whether their "zeta factor" $\zeta_i = \omega_i\tau^*$ is larger or smaller than unity. If the coupling is strong, that is, if $B > 0.5$, as it was in the example treated in ref 21, the most strongly coupled mode, generally the O···O or N···N mode of the hydrogen bond, tends to become "fast". Since, as pointed out, we need to evaluate the time-retarded integrals with the exponential kernels intact, which requires finding an adequate approximate instanton solution, we choose this solution by treating this most important mode in the adiabatic approximation and the other, more weakly coupled modes in either the adiabatic or sudden approximation, according to their zeta factors. In ref 21 we derived such an approximate instanton solution in the general case of a quartic potential coupled to an arbitrary number of symmetric modes; we termed it the "rainbow" solution because it handles a wide range of vibrational frequencies. Taking advantage of a specific conversion property of this solution, the time-retarded integrals were transformed into simple quadratures. As a result, the nonlocal part $\tilde{S}^0_{nl,s}$ of the instanton action in eq 5 was obtained in the form of a sum over 1D integrals which are easily evaluated numerically. The specific form of $\tilde{S}^0_{nl,s}$ is given by eq A.12 in the Appendix, in which the parameters used are defined. All the parameters in eqs 3−5 needed for the evaluation of the tunneling splitting are thus generated from calculated data, as detailed in the Appendix.

4. MULTIPLE-PROTON TRANSFER

As is clear from the previous section, the quality of the results obtained with the rainbow approximation depends on our ability to find an adequate approximate instanton solution $Q^0(\tau)$, that is, a solution that allows us to deal effectively with the troublesome nonlocal action. The compounds treated in the present study are all characterized by strong coupling, as follows from Table 1 in which $B_s \geq 0.6$. The simplest situation in this case arises when the coupling is dominated by a single mode. This is the case for MA, the example treated previously,[21] where $B \approx 0.7$ and is dominated by a single mode whose frequency ω_d (dimensionless, scaled by Ω) falls within the adiabatic range, since its zeta-factor $\zeta_d = \omega_d\tau^*$ is larger than 1 (see eq A.9). In this situation, we can follow the "standard" rainbow procedure of ref 21; this is generally the case for single-proton transfer along a hydrogen bond. For the compounds studied here, as expected for multiple-proton transfer, the symmetric coupling tends to be distributed over several modes whereby their components $B_{i=s}$ are smaller and/or the modes are outside the adiabatic range. There is a simple way to deal with this situation: substitute a single "effective" mode for the group of coupled symmetric modes by replacing the multimode kernel in the nonlocal action by an effective single-mode kernel. This remarkable property of systems with strong symmetric coupling is illustrated in Figure 1, in which

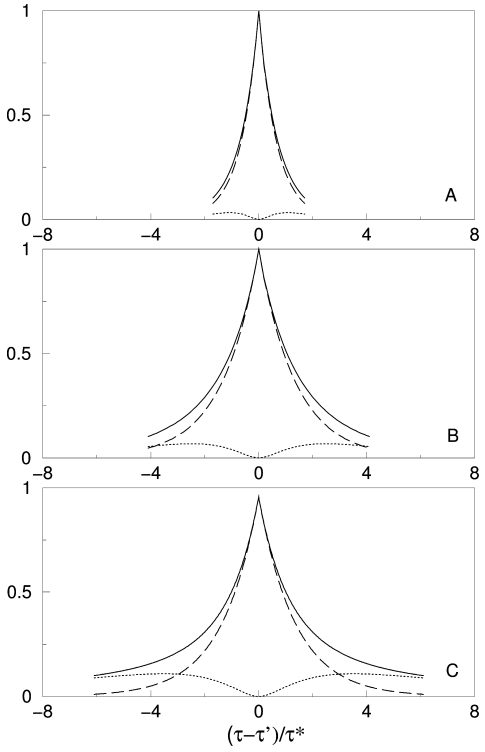

Figure 1. Illustration of the correspondence between the kernels of the (symmetric) nonlocal action defined in eq A.13: the solid and dashed lines depict the actual multimode kernel U_s and the effective-mode kernel U_{eff}, respectively, for malonaldehyde(H) (panel A), 2PH-2PY(HH) (panel B), and CLX(4H) (panel C). The kernels are scaled by their maximum at zero and are printed as a function of $(\tau - \tau')/\tau^*$, where τ^* is the characteristic time of tunneling defined in eq A.11. Along the abscissa U_s ranges from 1 to 0.1. The dotted line depicts the deviation $\Delta U = U_s - U_{eff}$; note that this deviation is small in the central area where U_s is significant, so that when it reaches its maximum, U_s has fallen off to ≤20% of its maximum for all the compounds listed in Tables 3 and 4

dx.doi.org/10.1021/jp4073608 | J. Phys. Chem. A XXXX, XXX, XXX−XXX

we compare the actual MD kernel with the effective-mode kernel for three sets of parameters, corresponding to the compounds in Table 1. In the Appendix, we show how the frequency ω_{eff} of the effective mode can be evaluated from the system parameters. The results in Figure 1A are based on data calculated for MA,[21] for which the deviation between the actual and "effective-mode" kernel is very small in the region where the MD kernel is large. Figure 1B is based on data calculated for 2PH-2PY, to be treated in the next section. In this complex there is a dominant mode, but its frequency is below the adiabatic range. The deviation between the two kernels is larger, but again occurs mainly in the wings in which the kernel is small. Therefore the effective-mode approach is clearly appropriate in this case. It remains a useful approximation even for CLX, also treated in the next section, although the coupling is not only weaker but also spread over more modes, as illustrated in Figure 1C. Hence, provided the coupling is strong, we can always apply the RIM to multiple-proton transfer by introducing the effective-mode approximation, which reduces the MD system to an effective 2D system defined by just two parameters, B_s and ω_{eff}, similar to the case of single-proton transfer.

Application of the RIM to a 2D system with a given B_s yields the instanton action in the form of $S_I(\omega)$ for the whole range of ω. For any of our MD systems one can then obtain an estimate of the instanton action as $S_I(\omega = \omega_{eff})$. For MA, where the dominant mode frequency ω_d as well as its approximation ω_{eff} are within the adiabatic range, this yields a tunneling splitting that is very close to the standard, namely, the MD result, as expected from the results in Figure 1A. For the multiple-proton transfer systems in Table 1, the deviations will be larger. However, whenever there is a dominant mode with a frequency of $\omega_d \sim \omega_{eff}$ within the adiabatic range, we can use the standard approach. Only when this frequency falls below this range, namely, when $\omega_{eff} < 1/\tau^* = (1 - B_s)^{1/2}$, we need to use the effective-mode approach. In that case we apply the interpolation procedure of ref 21, in which we showed how for such systems the instanton action can be obtained by linear interpolation between the rainbow limits. For a MD system this means linear interpolation between the corresponding limits $\tilde{S}_{nl,U}$ and $\tilde{S}_{nl,L}$ of the nonlocal action [defined after eq (A.12) of the Appendix], the former obtained for $\omega_{eff} = 1/\tau^*$ and the latter for $\omega_{eff} \ll 1$. The nonlocal action $\tilde{S}^0_{nl,s}$ in eq 5 is then approximated by the interpolated action at frequency ω_{eff}; this yields eq 6:

$$\tilde{S}^0_{nl,s} = \tilde{S}_{nl,L} + \zeta_{eff}[\tilde{S}_{nl,U} - \tilde{S}_{nl,L}] \quad (6)$$

where $\zeta_{eff} = \omega_{eff}\tau^*$. A similar procedure applies to the asymmetric term ΔS_a, but we omit those details here since this term is small and insignificant for the present systems.

Since this approach is clearly more approximate than the standard approach, it is useful to pay special attention to the case in which the effective-mode frequency is very close to the adiabatic limit, namely, when $\omega_{eff} \simeq 1/\tau^*$. In that case one can do better, since one can obtain the nonlocal action in the two limits for this mode: one that evaluates $Q^0(\tau)$ by treating it as a fast mode, and the other by treating it as a slow mode. Taking the average will generally yield a result that is more accurate than the effective-mode value. This "hybrid" approach is also useful if there are two strongly coupled modes with very different frequencies such that one is inside and the other is outside the adiabatic range. In that case, one treats both modes first as fast and then as slow and then averages the result. To decide which of the other modes are fast or slow, a different criterion applies for the fast and the slow calculation, depending on the relative values of ω_d and ω_{eff}; for the fast calculation the larger frequency should be smaller and for the slow calculation the smaller frequency should be larger than $1/\tau^*$.

These three approaches, standard, effective-mode, and hybrid, cover all of the situations represented by the four systems and their isotopomers to be considered here and should indeed cover most situations one is likely to encounter for systems with hydrogen bonds. To choose the approach to be used for a given system, one needs three quantities: the frequencies ω_d, ω_{eff}, and $1/\tau^*$ (all expressed in terms of the scaling frequency Ω). If $\omega_d \simeq \omega_{eff} > 1$, that is, if the coupling is dominated by a single symmetric mode in the adiabatic range, the standard approach applies. If $\omega_d \simeq \omega_{eff} < 1$, that is, if the dominant mode is below the adiabatic range, the effective-mode approach is indicated, but when $\omega_d \simeq \omega_{eff} \simeq 1$, the hybrid approach is preferable. If ω_d and ω_{eff} are quite different, a wide range of possibilities opens, but we will consider only the case in which the most strongly coupled mode is within the adiabatic range and one other strongly coupled mode is below this range. Under these conditions, the former mode will dominate the local coupling, but the latter may dominate the nonlocal kernel. This case therefore calls for the hybrid approach. In the next section all three approaches are illustrated by examples.

5. APPLICATION TO SPECIFIC HYDROGEN-BOND COMPOUNDS

5.1. General. The four compounds to be discussed, each with two or more hydrogen bonds engaged in proton tunneling are: FAD, BAD, the 2PH-2PY complex, and CLX. For all these compounds, as well as for some of their deuterium isotopomers, relevant experimental data are available. Using the RIM, we calculate the zero-point tunneling splittings. For FAD, BAD, and 2PH-2PY, these calculations are based on previously reported quantum-chemical data. For CLX we use newly calculated data detailed in section 5.5. Relevant results from these calculations are listed in Table 1, together with the corresponding data for MA used in ref 21, listed here for the sake of comparison. In addition to the adiabatic barrier height $V_{ad}(0)$ and the half-width Δx, change of the O···O (or N···N, etc.) separation between the EQ and the TS, and the frequency ω_0 of the tunneling mode in the EQ, we list four properties readily derived from the data: the crude-adiabatic barrier height V_0 and the scaling frequency Ω, whose ratio defines the scaling coefficient in eq 5, and the symmetric and antisymmetric coupling parameters B_s and B_a, respectively. As expected, the adiabatic barrier height increases roughly linearly with the number of hydrogen bonds broken during the transfer; the barrier width increases roughly as the square root of the number of those broken bonds. In all cases the symmetric coupling is strong and dominated by the symmetric stretching mode of the hydrogen bridges, and the antisymmetric coupling is very weak.

To implement the method, we have generated a code[29] based on input parameters such as those listed in Table 1 (and in Tables 2 and 5−7), which performs these calculations automatically by using the criteria discussed in the preceding section to choose the approach appropriate for the system at hand. The code treats also isotopomers with one or more protons replaced by deuterons, on the basis of the same

dx.doi.org/10.1021/jp4073608 | J. Phys. Chem. A XXXX, XXX, XXX−XXX

Table 2. Parameters of Symmetric and Antisymmetric Normal Modes of the Transition State Configuration Contributing to the Linear Coupling in Three Isotopes of FAD[a]

isotope	frequencies ω_i, cm^{-1}	displacements Δy_i, Å amu$^{1/2}$	B_i[b]	α_i[c]	ζ_i[d]	symmetry
HH	**520**	**1.34**	**0.53**	**0.50**	**1.00**	**s**
	750	0.38	0.09	0.06	1.43	s
	1402	0.11	0.03	0.01	2.68	s
	224	0.85	0.04	0.09	0.43	a
HD	**520**	**1.33**	**0.51**	**0.41**	**1.16**	**s**
	733	0.42	0.10	0.06	1.64	s
	224	0.88	0.04	0.08	0.50	a
DD	**519**	**1.32**	**0.51**	**0.36**	**1.34**	**s**
	718	0.47	0.12	0.06	1.85	s
	1248	0.13	0.03	0.01	3.22	s
	223	0.90	0.04	0.07	0.58	a

[a]Data for the dominant coupling mode are in bold font; only modes with $B_i \geq 0.02$ are listed. [b]Dimensionless coupling parameters defined in eq A.6. [c]Dimensionless kernel coefficients defined in eq A.2. [d]Dimensionless zeta factors defined in eq A.11.

quantum-chemical input. The results of the calculations are compared with those of other methods where available. Throughout the paper they are also compared to the earlier results obtained with the AIM; to assist the reader with this comparison, a simplified account of the approximations involved in each method has been added in a subsection of the Appendix.

5.2. Application to the Formic Acid Dimer. Along with MA, the FAD is serving as a benchmark for the calculation of tunneling splittings, following the measurements of Havenith et al.[3,4] on $(DCOOH)_2$ and $(HCOOH)_2$, which turned out to be even more informative than those on malonaldehyde and malonaldehyde-d_1, since they gave rise to tunneling splittings not only of the zero-point level but also of a vibrationally excited level. After some initial confusion, as narrated in ref 4, it turned out unexpectedly that the splitting is smaller for the excited level than for the ground level, as predicted correctly by our early AIM/DOIT calculation.[13] A second surprise was the observation[4] that in $(HCOOH)_2$, but not in $(DCOOH)_2$, the splitting of the excited level has the "wrong" sign with the minus level below the plus level, which could only be explained by the occurrence of a statistically improbable accidental resonance with another, as yet unidentified ro-vibrational level.[4,33] However, this complication does not affect the zero-point splitting.

The input data of the FAD in Table 1 are based on MC-QCISD/3-level calculations reported earlier.[13] The force-field parameters for the rainbow calculations are summarized in Table 2, in which the parameters of the dominant mode for the HH, HD, and DD isotopomers are listed in bold. It follows from these data and from the calculated intermediate parameters listed in Table 3 that the standard rainbow approach applies to the HD and DD isotopomers, but that the HH isotopomer, the one for which the splitting has been measured, requires the hybrid approach. The calculated splitting equals 540 MHz (0.018 cm^{-1}); the observed splitting of 474 MHz (0.0158 cm^{-1}) is close to the value obtained with the AIM/DOIT program,[13] namely, 450 MHz (0.015 cm^{-1}). The results for the isotopomers, for which no measurements are available, are listed in Table 4.

The early calculations not based on instanton techniques[5−8] produced conflicting results, which later proved to be wide off the mark. An early instanton calculation by Loerting and Liedl,[9] reported before the observed splitting was available, produced a result of 2700 MHz. This result was revised by Tautermann et al.,[10] following the publication of the ambiguous experimental data of ref 3, to 66 MHz. A subsequent quantum dynamics calculation by Luckhaus[11] yielded a splitting of 39 MHz, while a high-level instanton calculation by Mil'nikov et al.[12] yielded 114 MHz. None of these methods produced a value approaching the accuracy of our AIM calculation; note that all these results, including our own, were obtained before the correctly assigned experimental splitting of ref 4 was known. All these other methods are, moreover, computationally more demanding than the AIM (and the RIM).

Table 3. Dimensionless Parameters for Systems in Which the (Weak) Antisymmetric Coupling Is Incorporated in the (Rescaled) Parameters for Symmetric Coupling[a]

compound	$\tilde{B}_s$	$1/\tau^*$	ω_d	ζ_d	ω_{eff}	ζ_{eff}	rainbow approach
MA-H	0.71	0.54	0.67	1.25	0.81	1.51	standard
-D	0.71	0.53	0.88	1.65	1.03	1.93	standard
FAD-HH	0.70	0.55	0.55	1.00	0.60	1.09	hybrid
-HD	0.69	0.55	0.65	1.17	0.71	1.28	standard
-DD	0.70	0.55	0.73	1.34	0.80	1.46	standard
BAD-HH	0.63	0.61	0.73	1.19	0.47	0.76	hybrid
-HD	0.62	0.61	0.87	1.42	0.56	0.91	hybrid
-DD	0.63	0.61	0.98	1.62	0.63	1.04	hybrid
2PH-2PY-HH	0.64	0.60	0.40	0.66	0.45	0.74	effective-mode
-DH	0.64	0.60	0.44	0.73	0.49	0.82	effective-mode
-HD	0.63	0.60	0.51	0.84	0.57	0.95	effective-mode
-DD	0.64	0.60	0.54	0.90	0.61	1.02	hybrid
CLX-4H	0.58	0.64	0.44	0.68	0.47	0.74	effective-mode

[a]$\tilde{B}_s$ is the collective coupling parameter; $1/\tau^* = (1 - \tilde{B}_s)^{1/2}$ the characteristic (dimensionless) frequency of motion under the adiabatic barrier; and $\zeta = \omega\tau^*$. Subscripts d and eff refer to the dominant coupling mode and the effective mode, respectively. MA refers to malonaldehyde treated in ref 21. The last column specifies which rainbow approach is used for the evaluation of the tunneling splittings listed in Table 4.

5.3. Application to the Benzoic Acid Dimer. The benzoic acid dimer (BAD) shows a tunneling splitting of 1107 ± 8 MHz (0.0369 cm^{-1}),[17] measured as the difference between the splittings in the electronic ground state and the lowest singlet excited state. In the excited state the excitation is essentially localized in one of the benzene rings, and the two

dx.doi.org/10.1021/jp4073608 | J. Phys. Chem. A XXXX, XXX, XXX−XXX

Table 4. Calculated Dimensionless Parameters Used In Equations 3−5 To Evaluate The Zero-Point Tunneling Splitting ΔE_0[a]

molecule	$\tilde{S}_{ad}$	$\tilde{S}^{(0)}_{nl,s}$	C_a	ΔS_a	S_I	ΔE_0^{calc}	ΔE_0^{obs}
MA-H	1.01	0.24	1.01	0	6.62	25.2	21.6
-D	1.01	0.19	1.01	0	8.42	3.4	2.9
FAD-HH	1.04	0.31/0.08	0.98	0.34/0.15	14.37	0.018	0.0158[b]
-HD	1.04	0.27	0.98	0.31	18.37	3.2×10^{-4}	
-DD	1.03	0.24	0.98	0.29	20.45	3.5×10^{-5}	
BAD-HH	1.15	0.25/0.13	0.99	0.32/0.23	14.06	0.022	0.0369[c]
-HD	1.16	0.22/0.22	1.00	0.25/0.25	16.66	1.6×10^{-3}	
-DD	1.15	0.19/0.19	1.00	0.22/0.22	18.40	2.4×10^{-4}	
2PH-2PY-HH	1.13	0.29	1.02	0.11	14.84	0.011	0.0176[d]
-DH	1.13	0.29	1.03	0.11	16.25	2.5×10^{-3}	2.1×10^{-3}[,d]
-HD	1.13	0.29	1.04	0.06	18.10	3.6×10^{-4}	$<3.3 \times 10^{-4}$[,d]
-DD	1.13	0.19	1.02	0.06	18.24	2.8×10^{-4}	$<3.3 \times 10^{-4}$[,d]
CLX-4H	1.21	0.23	1.00	0.12	26.42	1.4×10^{-7}	$\sim 3 \times 10^{-7}$[,e]

[a] $\tilde{S}_{ad}$ and $\tilde{S}^0_{nl,s}$ represent the main and the nonlocal parts of $\tilde{S}_{I,s}$ in eq 5, respectively; C_a and ΔS_a represent the (weak) antisymmetric coupling; S_I is the total instanton action. The double numbers in columns 3 and 5 refer to the two limiting values in cases where the hybrid approach is used (see Table 3). The calculated and observed splittings in columns 7 and 8 are in cm^{-1}. The data for malonaldehyde (MA) are taken from ref 21. [b] Reference 4. [c] Reference 17. [d] References 18 and 20. [e] ΔE_0^{obs} is an estimate based on k_r ($T = 0$) in the solid from ref 28.

Table 5. Parameters of Symmetric and Antisymmetric Normal Modes of the Transition State Configuration Contributing to the Linear Coupling in Three Isotopes of BAD[a]

isotope	frequencies ω_i, cm^{-1}	displacements Δy_i, Å $amu^{1/2}$	B_i[b]	α_i[c]	ζ_i[d]	symmetry
HH	199	1.89	0.19	0.41	0.40	s
	579	**0.69**	**0.22**	**0.16**	**1.15**	**s**
	718	0.43	0.13	0.08	1.43	s
	294	0.56	0.04	0.05	0.58	a
HD	199	1.89	0.19	0.34	0.46	s
	579	**0.69**	**0.21**	**0.13**	**1.35**	**s**
	702	0.24	0.04	0.02	1.63	s
	712	0.37	0.09	0.05	1.66	s
	293	0.57	0.04	0.05	0.68	a
DD	199	1.89	0.19	0.31	0.54	s
	579	**0.68**	**0.21**	**0.12**	**1.56**	**s**
	699	0.46	0.14	0.06	1.89	s
	293	0.58	0.04	0.04	0.79	a

[a] Data for the dominant coupling mode are in bold font; only modes with $B_i \geq 0.04$ are listed. [b] Dimensionless coupling parameters defined in eq A.6. [c] Dimensionless kernel coefficients defined in eq A.2. [d] Dimensionless zeta factors defined in eq A.11.

protons are inequivalent; because this will weaken the hydrogen bonding, it is plausible to assign the splitting predominantly to the ground state. This is the assignment we adopted in our earlier AIM/DOIT calculation.[14] Since our calculation is restricted to the B3LYP/6-31+G* level, the assignment should be accurate enough for the present purpose. The earlier calculation yielded a zero-point splitting of 1920 MHz (0.064 cm^{-1}), a value that exceeds the observed splitting by a factor 1.7. If in the FAD the splitting is calculated at this level, it is also too large, namely by a factor 1.2. Using the same PES, we repeat the calculation here with the RIM. The force-field parameters are summarized in Table 5, in which the dominant modes for the HH, HD, and DD isotopomers are listed in bold. It follows from these data and the calculated intermediate parameters listed in Table 3 that the standard rainbow approach does not apply since there is a second strongly coupled mode of a much lower frequency, well below the adiabatic range. This mode, with a frequency of 199 cm^{-1} (ζ_d = 0.40), has a large α_i coefficient, as defined in eq A.2, which means that it has a strong effect on the nonlocal term. Therefore the calculation of the splitting requires the hybrid approach. This results in a splitting of 660 MHz (0.022 cm^{-1}), a result too low by a factor of 1.7. The results for the isotopomers, for which no measurements are available, are listed in Table 4. It would be interesting to compare our results with those of other theoretical methods, but no such calculations have been reported thus far; given the size of the BAD, we expect some of these calculations to be very laborious.

Zero-point tunneling splittings have also been observed in doped BAD crystals. In neat crystals the site symmetry introduces asymmetry in the transfer potential, which prevents the observation of tunneling splitting. However, in crystals doped with thioindigo and selenoindigo, zero-point tunneling matrix effects of 8.4 and 6.5 GHz, respectively, have been measured;[34,35] presumably, these matrix element occur due to the BAD molecules adjacent to the dopants. The values, which may be taken as rough estimates for the tunneling splitting, are much larger than those in the gas phase. This is thought to be mostly due to the shorter O···O distance and the corresponding lower barrier in the crystal, where the paired monomers are squeezed by crystal forces. While these observations cannot be used at this time to compare different tunneling approaches, they are important for the study of compounds that cannot be

dx.doi.org/10.1021/jp4073608 | J. Phys. Chem. A XXXX, XXX, XXX−XXX

studied in the gas phase. We return to this problem in section 5.5.

5.4. Application to 2-Pyridone-2-hydroxypyridine. The dimeric complex 2-pyridone-2-hydroxypyridine (2PH-2PY), illustrated in Figure 2, is bound by an O···H−O and an N−H···N hydrogen bond. Transfer of the protons in these two bonds gives rise to the interchange of the two molecules. The observation of a tunneling splitting of 530 MHz (0.0176 cm^{-1})[18] in a cold beam indicates proton exchange between equivalent sites, which means that the two protons move simultaneously. The subsequent observation of a large isotope effect,[19,20] as indicated by the splittings of 63 MHz (2.1×10^{-3} cm^{-1}) for the DH (with an O−D−O hydrogen bond) and ≤10 MHz (3×10^{-4} cm^{-1}) for the HD and DD isotopomers, shows clearly that the double-proton transfer proceeds by tunneling. Originally, the splitting, observed as the difference between the splittings in the ground and excited states, as in BAD, was assigned to the excited state,[18] but for basically the same reason as in BAD, this assignment was subsequently reversed.[19,20] The AIM/DOIT calculations on the ground-state PES, based on a potential calculated at the B3LYP/6-31++G(d,p) level, yielded a single transition state corresponding to a concerted double-proton transfer. The corresponding splittings of 1240, 129, 36, and 10 MHz (414, 43, 12, and 3.3×10^{-4} cm^{-1}) obtained for the four isotopomers investigated are in reasonable agreement with the observed splittings.

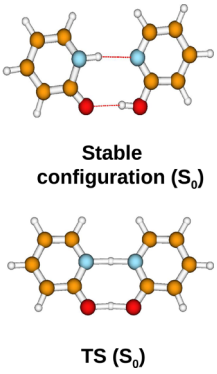

Figure 2. Structure of the stable and transition state configuration of the 2-pyridone-2-hydroxy-pyridine complex in the ground state.

The present rainbow calculations are based on the same potential. The relevant force-field parameters are summarized in Table 6, where the dominant mode for the HH, DH, HD, and DD isotopomers is printed in bold. It strongly dominates the coupling, but its frequency of 332 cm^{-1} ($\omega_d = 0.40$) is well below $1/\tau^*$ ($\zeta_d = 0.74$), except for the DD transfer for which $\zeta_d \approx 1$; this indicates that the effective-mode approach should be used. As expected, the effective-mode frequency, listed in Table 3, is close to the dominant-mode frequency, but slightly higher (374 vs 332 cm^{-1}). For the DD isotopomer a hybrid approach is indicated. The calculated splittings for the observed HH and DH transfers, and for the unobserved HD and DD transfers are 330, 75, 11, and 8.4 MHz (110, 25, 3.6, and 2.8×10^{-4} cm^{-1}), respectively; they thus are somewhat more accurate than the AIM/DOIT results.

5.5. Application to Calix[4]arene. The molecule of calix[4]arene (CLX), illustrated in Figure 3, is of special interest in this context, because of its 4-fold symmetry allowing simultaneous transfer of four protons. The early attempts to study low-temperature proton transfer in solid calixarenes by NMR techniques similar to those applied to BAD did not give rise to reliable results.[36,37] Recently, Ueda and Oguni[28] used calorimetric and dielectric relaxation methods for this purpose and obtained clear evidence for proton tunneling in solid CLX. They observed a striking difference between the two isotopomers with respect to the temperature dependence of the rates of spontaneous enthalpy release and absorption on intermittent heating. The deuterated compound showed a hysteresis pattern typical for a glass transition, but in the undeuterated compound the hysteresis signal had a much larger width and amplitude and was shifted to much lower temperatures (50−120 K instead of 140 ± 3 K). They ascribed this phenomenon to proton rearrangement among the four hydroxyl groups. Since no corresponding deuteron rearrangement is observed, they assigned it to tunneling and estimated

Table 6. Parameters of Symmetric and Antisymmetric Normal Modes of the Transition State Configuration Contributing to the Linear Coupling in Four Isotopes of 2PH-2PY[a]

isotope	frequencies ω_i, cm^{-1}	displacements Δy_i, Å $amu^{1/2}$	B_i[b]	α_i[c]	ζ_i[d]	symmetry
HH	158	1.35	0.06	0.16	0.30	s
	332	**1.58**	**0.36**	**0.46**	**0.63**	**s**
	691	0.40	0.09	0.06	1.31	s
	897	0.20	0.04	0.02	1.70	s
DH	158	1.35	0.06	0.15	0.33	s
	332	**1.58**	**0.34**	**0.42**	**0.69**	**s**
	690	0.39	0.09	0.05	1.43	s
	896	0.21	0.04	0.02	1.86	s
HD	158	1.35	0.05	0.12	0.37	s
	331	**1.59**	**0.33**	**0.36**	**0.78**	**s**
	691	0.40	0.09	0.05	1.64	s
	895	0.20	0.04	0.01	2.12	s
DD	157	1.35	0.06	0.12	0.41	s
	331	**1.58**	**0.34**	**0.34**	**0.87**	s
	690	0.39	0.09	0.04	1.80	s
	894	0.20	0.04	0.01	2.34	s

[a]Data for the dominant coupling mode are in bold font; only modes with $B_i \geq 0.04$ are listed. [b]Dimensionless coupling parameters defined in eq A.6. [c]Dimensionless kernel coefficients defined in eq A.2. [d]Dimensionless zeta factors defined in eq A.11.

dx.doi.org/10.1021/jp4073608 | J. Phys. Chem. A XXXX, XXX, XXX−XXX

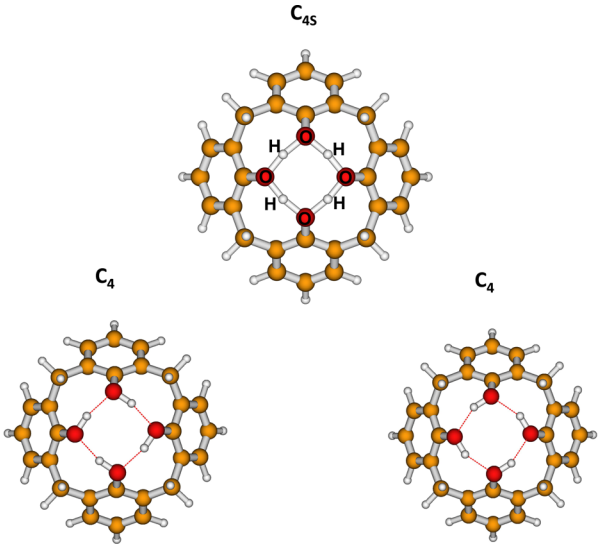

Figure 3. Structure of calix[4]arene in the two equivalent equilibrium configurations (left and right). The scheme in the center depicts the structure and the hydrogen-bond configuration of the transition state.

the rearrangement rate $k_r(T)$ by following the enthalpy relaxation after a sudden jump in the sample temperature. While the temperature dependence of k_r could be represented by a single activation energy of about 11 kcal/mol for CLX-d_4, the corresponding activation energy of 10 kcal/mol for CLX was observed only at temperatures above 200 K. At lower temperatures the activation energy gradually diminished and vanished completely below 100 K, a pattern that represents a curved Arrhenius plot, as is typical for tunneling. The limiting relaxation rate k_r at $T < 100$ K, estimated to be about 10^{-4} s^{-1}, was interpreted to be the zero-point tunneling rate $k_r(0)$.

This picture is very similar to that observed in BAD crystals, except that the rate is slower by a factor of about 10^{12}. Since, as pointed out in ref 28, the BAD and CLX lattices show similar properties, including O···O separations of 2.62−2.65 Å and double-well asymmetries of about 60 cm^{-1}, one expects the relation between $k_r(0)$ and the zero-level splitting ΔE_0 to be about the same in both lattices. Since the rate is a quadratic function of the splitting, this means that the splitting in CLX should be a factor of about 10^{-6} smaller than that in BAD. From the measurements on BAD crystals doped with thioindigo, a zero-level splitting of 8.4 GHz has been estimated,[35] which leads to an estimate of about 8 kHz (3×10^{-7} cm^{-1}) for CLX.

To calculate the tunneling splitting, we generated the input data from new calculations at the B3LYP/6-31G* level. As the parameter values in Table 1 indicate, the barrier turns out to be considerably higher and wider than that of the three compounds treated above, which is to be expected since there are twice as many hydrogen bonds to break. The force-field parameters are summarized in Table 7, where the dominant mode is shown in bold. It dominates strongly, but its frequency of 438 cm^{-1} is well below the adiabatic limit ($\zeta_d < 1$), so that the effective-mode approach is indicated. As shown in Table 3, the effective-mode frequency is slightly higher, namely 470 cm^{-1} (0.47 vs 0.44 in dimensionless units). The calculated zero-point splitting listed in Table 4 is 4 kHz or about 1.4×10^{-7} cm^{-1}, for the isolated molecule, in satisfactory agreement with the experimental estimate. Unlike BAD, the crystal forces in CLX are not aligned with the tunneling direction, so that no strong difference is expected between the single molecule and the solid state results. The method of calculation implies the prediction of a very large isotope effect, which we have not pursued in detail since it is unlikely to be observable in the near term.

The only comparable systems previously considered are the tetramers of water and alcohols for which, however, no relevant experimental data are available. The calculations by Vener and Sauer[38] on the methanol tetramer, based on a diagonalization procedure, yielded a zero-point splitting reported as ≪0.1 cm^{-1}, which, in view of our results on CLX, should be correct but is tantamount to the admission that their method cannot deal with such small splittings. The only quantitative result reported refers to a vibrationally excited level and is thus not relevant for the present purpose.

This concludes our report on the application of the rainbow approach to proton transfer in hydrogen-bond systems with multiple-proton tunneling. Compared to the AIM/DOIT approach, which is also based on only stationary structures, RIM is more rigorous, which allows more control over the approximations used. The calculations can be simplified to a one-step procedure in which the decision of how to deal with a variety of coupled modes, symmetric and antisymmetric, weak and strong, slow and fast, is taken automatically by the code.[29] In this respect, the rainbow code is also more robust and more

Table 7. Parameters of Symmetric and Antisymmetric Normal Modes of the Transition State Configuration Contributing to the Linear Coupling in CLX-4H[a]

frequencies ω_i, cm^{-1}	displacements Δy_i, Å amu$^{1/2}$	B_i[b]	α_i[c]	ζ_i[d]	symmetry
83	2.16	0.02	0.12	0.13	s
319	0.54	0.02	0.03	0.49	s
335	0.86	0.05	0.08	0.51	s
438	**1.05**	**0.13**	**0.16**	**0.67**	**s**
601	0.51	0.06	0.05	0.92	s
694	0.60	0.11	0.08	1.06	s
840	0.32	0.04	0.03	1.28	s
876	0.27	0.04	0.02	1.34	s
1303	0.15	0.02	0.01	1.99	s
1381	0.14	0.02	0.01	2.11	s
282	0.51	0.01	0.02	0.43	a

[a]Data for the dominant coupling mode are in bold font; only modes with $B_{i=s} \geq 0.02$ are listed. [b]Dimensionless coupling parameters defined in eq A.6. [c]Dimensionless kernel coefficients defined in eq A.2. [d]Dimensionless zeta factors defined in eq A.11.

dx.doi.org/10.1021/jp4073608 | J. Phys. Chem. A XXXX, XXX, XXX−XXX

user-oriented than the DOIT code, which requires occasional input from the operator since the approximations are not automatically controlled by the code. On the other hand, AIM has the merit of being able to deal with the splittings of excited levels. At any rate, it is useful to have more than one method to deal with these complicated systems. To the best of our knowledge, there is no other method of this kind that has been tested for a series of molecules and complexes with a range of zero-point splittings.

Finally, we relate the basic features of concerted multiple-proton tunneling, studied here, to those of the more familiar single-proton transfer, namely those of the extensively studied proton transfer in MA. In all the systems reported here, and in MA which we reported in ref 21, the tunneling splitting is due to proton exchange along hydrogen bonds, in which the tunneling is strongly promoted by hydrogen-bridge modes. This is illustrated in Table 1 by the significant shortening of the hydrogen-bridge length from EQ to minimum energy path. In the literature such effects are usually associated with "corner cutting", which measures the deviation of the instanton from the TS. Since our method avoids the laborious evaluation of the instanton path, it does not immediately reveal the amount of corner cutting. This effect is strong if the coupled mode is "slow" on the time scale of tunneling; it is therefore clear that it should be relatively weak in all compounds listed in Table 1, since those compounds are (mostly) close to the opposite, adiabatic limit. As argued throughout the present study, this is a consequence of the strong symmetric coupling which scales down the imaginary frequency under the adiabatic barrier, shifting the hydrogen-bridge mode to the "fast" range; correspondingly, the skeletal movement between the EQ and TS structures, illustrated in Table 1, follows the proton almost adiabatically. The trend revealed by this change of geometry shows that the compounds treated in the present study share the same dynamics features typical for MA. Indirectly, the amount of corner cutting, measured as the "depth" of penetration of the instanton into the nonadiabatic "enclave", can still be estimated in our approach as follows: if the whole distance between the TS and the linear path that connects the minima is taken as unity, then this depth is roughly given by the ratio of the nonlocal part of the instanton action to the main part corresponding to the adiabatic barrier. As seen from the first two columns of Table 4, this ratio is in the range of 0.17–0.25.

6. CONCLUSION

This study forms part of a continuing search for a practical method to analyze proton dynamics in polyatomic systems, including systems of biological interest, in which protons often transfer along hydrogen bonds and in pairs. In particular, it provides a test of the ability of the RIM, as newly developed in ref 21, to match the observed zero-point tunneling splittings in four compounds in which protons move concertedly in pairs or quartets along hydrogen bonds. Since it is based on a Hamiltonian derived from only two stationary quantum-chemical structures and harmonic force fields, and yields also isotope effects, the method is more efficient than the conventional methods based on the evaluation of the instanton path by direct minimization of the Euclidian action, without significant loss of accuracy. As the comparisons reported in Sec. 5 show, both the RIM and the AIM yield results for the FAD, the only example of concerted multiple-proton transfer for which such a comparison can be made, that are superior to those obtained to date with other methods. The fact that none of these methods have been used thus far to deal with any of the other examples further supports the argument that our method is not only at least as accurate but also simpler to apply than these methods.

The success of our approach we ascribe to two factors: the direct implementation of the full symmetry inherent in systems showing tunneling splitting and the elimination from the outset of degrees of freedom that have an insignificant effect on this splitting. These two factors govern the form of the imaginary-mode Hamiltonian, its key feature being reflected in the name. Effective use of the symmetry imposes a formulation in terms of the transition state rather than the equilibrium configuration. Since the TS is the point of highest symmetry, it allows elimination of irrelevant degrees of freedom by the simple device of restricting the coupling between the tunneling motion and the harmonic normal modes to linear terms. Linear approximations are ubiquitous in theoretical models, their success being based not only on the expected smallness of higher-order terms, but also on the observation that in the case of many degrees of freedom such terms often are subject to mutual cancellation, which can indeed be shown to be the case for the present systems. While this truncation of the Hamiltonian undoubtedly leads to some loss of accuracy, it has the virtue of not requiring further major approximations, among which the novel way in which the relatively weak nonlocal interactions are calculated is the most significant. This stands in contrast to methods based on the evaluation of the instanton path, which start with a more complete Hamiltonian, but require additional approximations at a later stage in which the complexity of calculation makes it difficult to estimate their effect. This, at least, is our reading of the relative success of the RIM (and the AIM) compared to other methods that have been applied to concerted multiple-proton transfer.

APPENDIX

Summary of the Rainbow Approximation

The imaginary-mode Hamiltonian in the rainbow approach is generated in terms of the (mass-weighted) normal modes (x, $\{y\}$) of the TS configuration taken at zero, in the form of eq 1 of the main text. Introducing the dimensionless coordinates $Q = x/\Delta x$ and $q_i = y_i/\Delta x$, scaling energy by the height V_0 of the 1D potential $V_{1D}(x)$, and measuring frequencies ω_i and time τ in units of the scaling frequency Ω, the Hamiltonian takes the form

$$H = \frac{1}{2}\dot{Q}^2 + \frac{1}{2}\sum_i \dot{q}_i^2 + V(Q, \{q\});$$
$$V(Q, \{q\}) = V_{1D}(Q) + \sum_i \gamma_i \Lambda_i(Q) q_i + \frac{1}{2}\sum_i \omega_i^2 q_i^2 \quad (A.1)$$

where the dotted symbols are derivatives with respect to τ here and hereafter; $\Lambda_{i=a}(Q) = -Q$ and $\Lambda_{i=s}(Q) = -Q^2$, and the coupling constants γ_i are defined below. Higher-order coupling terms are not explicitly included in this Hamiltonian, but are partially accounted for by recalibrating the linear coupling constants γ_i, as detailed in ref 21.

The instanton action in eqs 3 and 4 of the main text is the Euclidean action S_E at $T = 0$, evaluated along the instanton trajectory, defined by the condition $\delta S_E = 0$. The corresponding equations for the q-coordinates, $\delta S_E/\delta q_i = 0$, correspond to forced harmonic oscillators and can be solved exactly; this

dx.doi.org/10.1021/jp4073608 | J. Phys. Chem. A XXXX, XXX, XXX–XXX

yields a quasi-1D instanton problem for the reaction coordinate, defined by the following relations:

$$S_E = \int_{-\infty}^{\infty} d\tau \left[\frac{1}{2}\dot{Q}^2 + V_{ad}(Q) + \int_{-\infty}^{\infty} d\tau' \dot{\Lambda}[Q(\tau')]\dot{\Lambda}[Q(\tau)]U(\tau - \tau') \right];$$
$$\delta S_E/\delta Q = 0;$$
$$U(\tau - \tau') = \sum_{i=a,s} \alpha_i \exp(-\omega_i|\tau - \tau'|); \quad \alpha_i = \gamma_i^2/4\omega_i^3 \tag{A.2}$$

This action consists of a dominant local term, which corresponds to 1D motion in the adiabatic potential $V_{ad}(Q)$, defined for eq A.1 from the condition $\partial V(Q,\{q\})/\partial\{q\} = 0$, and a smaller nonlocal term of the time-retarded interaction, which is positive and is governed by the multi-mode kernel $U(\tau - \tau')$.

To turn the quantities in eq A.2 into normal, dimensional units, the adiabatic potential $V_{ad}(x)$ needs to be evaluated. The barrier height $V_{ad}(0)$ is obtained from electronic structure calculations and its (mass-weighted) half-width Δx is given by eq A.3:

$$\Delta x = \sum_{\alpha=1}^{3}\sum_{j=1}^{N} \mathbf{M}_{\alpha,j}^{1/2}(X_{\alpha,j}^{R} - X_{\alpha,j}^{\ddagger})L_{\alpha,F}^{\ddagger} \tag{A.3}$$

where $\alpha = x, y, z$; N is the number of atoms; $\mathbf{M}$ is the $3N \times 3N$ diagonal matrix of masses; $X_{\alpha,j}^{R}$ and $X_{\alpha,j}^{\ddagger}$ are the Cartesian coordinates of the reactant and transition state, respectively; and $L_{\alpha,F}^{\ddagger}$ is the eigenvector of the mode with imaginary frequency at the transition state. The curvatures at the top and the bottom of the adiabatic potential are given by the respective frequencies along the reaction coordinate $|\boldsymbol{\omega}^*|$ and $\boldsymbol{\omega}_0$, where the latter is evaluated from the relation between the two sets of normal modes $(x,\{y\})$ of TS and $\{z\}$ of EQ, given by a unitary matrix $\mathbf{G}$ in the form

$$\boldsymbol{\omega}_0^2 = \sum_j \mathbf{G}_{0j}^2 \boldsymbol{\omega}_{0j}^2 \tag{A.4}$$

$\boldsymbol{\omega}_{0j}$ being the frequencies of the normal modes in the EQ. [This frequency also enters the pre-exponent $\mathcal{A}$ in the tunneling splitting in eq 4 in the main text.] In the intermediate region the potential should interpolate smoothly between the two stationary points, namely, between $Q = 0$ and $|Q| = 1$ in the dimensional units used. This is the only part needed in the instanton formalism, since it is a quasiclassical approach and all integrals run over Q, between the minima at $Q = \pm 1$. As argued in the main text, the potential shape in this region is well approximated by an analytical function of the quartic type, which in the present formulation yields

$$V_{ad}(Q) = (1 - B)(1 - Q^2)^2 \tag{A.5}$$

The reduction of the barrier height from V_0 (when the oscillators are frozen) to $V_{ad}(0)$ (when they are relaxed) by a factor $(1 - B)$ characterizes B as the main coupling parameter of the approach; it defines also the characteristic time of tunneling in eq A.2: $\tau^* = 1/(1 - B)^{1/2}$ (in units Ω). In general, B combines the contributions of the s- and a-modes, but for all compounds of interest in the present study it is dominated by the former. The corresponding quantities are defined as

$$B = B_a + B_s; \quad B_{a,s} = \sum_{i=a,s} B_i; \quad B_i = \gamma_i/2\omega_i^2;$$
$$B_a << B_s \tag{A.6}$$

The coupling constants γ_i which define B_i as well as the kernel coefficients α_i in eq A.2 are proportional to the displacements Δy_i of the oscillators between the TS and the EQ and are given by

$$\gamma_i = \boldsymbol{\omega}_i^2 \Delta y_i/\Delta x; \quad \Delta y_i = \sum_{\alpha=1}^{3}\sum_{j=1}^{N} \mathbf{M}_{\alpha,j}^{1/2}(X_{\alpha,j}^{R} - X_{\alpha,j}^{i})L_{\alpha,F}^{i} \tag{A.7}$$

where $L_{\alpha,F}^{i}$ is the eigenvector of the mode $\boldsymbol{\omega}_i$ at the transition state, in analogy with eq A.3. Similar to B, there are s- and a-components in the nonlocal term in eq A.2, defined as

$$S_{nl,s} = \int_{-\infty}^{\infty} d\tau \dot{\Lambda}_s \int_{-\infty}^{\infty} d\tau' \dot{\Lambda}_s U_s(\tau - \tau');$$
$$S_{nl,a} = \int_{-\infty}^{\infty} d\tau \dot{\Lambda}_a \int_{-\infty}^{\infty} d\tau' \dot{\Lambda}_a U_a(\tau - \tau') \tag{A.8}$$

These double-time integrals (τ,τ') over exponential kernels do not allow a general solution of the variational problem in eq A.2. The conventional approach, whereby these kernels are treated in the AA or SA, performs poorly for the compounds of interest because of the presence of strongly coupled s-modes for which $\omega_i\tau^*$ is close to unity. As seen from Table 1, B is in the range of ~0.6−0.7 and has only a weak antisymmetric component ($B_a \ll B_s$). The weak asymmetric coupling leads to (small) correction coefficients and (again insignificant) rescaling of the parameters of the symmetric coupling; this yields the instanton action in the form of eq 5 of the main text, where C_a and ΔS_a are the correction coefficients, and the tilde over the symbols of the remaining symmetric parameters reflects the rescaling. After this step, only symmetric coupling remains, so that we need to evaluate the action for the problem defined in eq A.2, but with symmetric coupling only, and with parameters carrying a tilde; below we omit the tilde for clarity.

The lengthening of $\tau^* = 1/(1 - B)^{1/2}$ with increasing B brings the most important coupled mode of the hydrogen bridge closer to the adiabatic limit; as a result, the s-mode part of the kernel in eqs A.2 and A.8 falls off rapidly, and $S_{nl,s}$ remains small even in the case of strong coupling. On the basis of this property, we can avoid approximating the kernels and instead use a properly chosen approximate instanton solution $Q^0(\tau)$ to evaluate $S_{nl,s}$. The instanton action resulting from eq A.2 then takes the form of eq 5 of the main text:

$$S_{I,s} = S_{ad} + S_{nl,s}^0; \quad S_{ad} = \int_{-\infty}^{\infty} d\tau \left[\frac{1}{2}\dot{Q}^2 + V_{ad}(Q) \right]$$
$$= (4/3)\sqrt{2(1 - B_s)};$$
$$S_{nl,s}^0 = \int_{-\infty}^{\infty} d\tau \dot{\Lambda}^0 \int_{-\infty}^{\infty} d\tau' \dot{\Lambda}^0 U_s(\tau - \tau') \tag{A.9}$$

where $\Lambda^0(\tau) = -[Q^0(\tau)]^2$. For a given solution $Q^0(\tau)$, the nonlocal term can be evaluated without approximations for the kernels, since the exponents $\exp(\mp\omega_i\tau)$ can be evaluated if we set $\tau = \tau(\Lambda^0)$, thus recasting $S_{nl,s}^0$ into the general form

dx.doi.org/10.1021/jp4073608 | J. Phys. Chem. A XXXX, XXX, XXX−XXX

$$S_{\mathrm{nl,s}}{}^{0} = \int d\Lambda^{0} \int d\Lambda'^{0} U_{\mathrm{s}}(\Lambda^{0}, \Lambda'^{0});$$
$$U_{\mathrm{s}}(\Lambda^{0}, \Lambda'^{0}) = \sum_{i=\mathrm{s}} \alpha_i \phi_i^{+}(\Lambda^{0}) \phi_i^{-}(\Lambda'^{0}) \tag{A.10}$$

The result of this approximation depends on whether an adequate approximate solution $Q^{0}(\tau)$ can be found. In the case of a hydrogen bond, the existence of such a solution and its nature are indictated by the presence of strongly coupled mode(s) of the hydrogen-bond bridges with a relatively high frequency, which may bring it close to the adiabatic limit, as discussed above. This suggests returning to eq A.2 and obtaining $Q^{0}(\tau)$ in the conventional way, that is, by treating this dominant mode in the AA, and treating the remaining weakly coupled modes in the AA or SA, depending on whether their zeta-factors

$$\zeta_i = \omega_i \tau^{*}; \quad \tau^{*} = 1/\sqrt{1 - B} \tag{A.11}$$

are larger or smaller than unity, respectively. In ref 21 we derived such an approximate instanton solution in the general case of $V_{1D}(Q)$ coupled to an arbitrary number of symmetric modes; it has a remarkable conversion property, as it is obtained in the form of the reverse function $\tau = \tau(Q^{0})$, so that the transformation A.10 follows naturally. If $V_{\mathrm{ad}}(Q)$ is in the form of the quartic potential of eq A.5, the evaluation of $S^{0}_{\mathrm{nl,s}}$ is further simplified, since for $\tau \geq 0$ the exponents of the kernels take the form $\exp(\mp\omega_i\tau) \equiv \phi_i^{\pm}(\bar{\Lambda})$, where the functions $\phi_i^{\pm}$ are *analytical* expressions of $\bar{\Lambda} = 1 - \bar{Q}^2$, $\bar{Q} = Q^{0}(\tau)/Q_0 \leq 1$ being the coordinate scaled by its boundary value: $Q_0 = Q^{0}(\tau \to \infty)$. The final result for the nonlocal action is thus obtained in form of simple quadratures (z denotes $\bar{\Lambda}$; $\bar{\Lambda}'$):

$$\tilde{S}_{\mathrm{nl,s}}{}^{0} = 2{Q_0}^{4} \sum_{\mathrm{i=s}} \tilde{\alpha}_i C(\phi_i^{\pm});$$
$$C(\phi_i^{\pm}) = -{I_{1i}}^{2}(0, 1) + \int_0^1 \mathrm{d}z[\phi_i^{+}(z) I_{2i}(z, 1)$$
$$+ I_{1i}(0, z)\phi_i^{-}(z)]; \quad I_{1i}(a, b) = \int_a^b \mathrm{d}z \phi_i^{+}(z);$$
$$I_{2i}(a, b) = \int_a^b \mathrm{d}z \phi_i^{-}(z) \tag{A.12}$$

where we have reinstated the tildes to indicate that corrected parameters should be used if antisymmetric coupling is present. This action has two limits: the upper limit denoted by $\tilde{S}_{\mathrm{nl,U}}$ is obtained if all the coupled modes in the derivation of $Q^{0}(\tau)$ are treated as "fast", and the lower limit denoted by $\tilde{S}_{\mathrm{nl,L}}$ is obtained if all the coupled modes are treated as "slow". These rainbow limits correspond to the collective slow-flip and fast-flip solutions, respectively.

Equation A.12 represents the rainbow approximation for $\tilde{S}_{\mathrm{nl,s}}$ in the case of the quartic potential A.5. Note that the numerical scheme is very efficient since the functions $\phi_i^{\pm}(z)$ are analytical expressions and the boundary value Q_0 is obtained from a simple numerical procedure, as detailed in ref 21. Finally, including the antisymmetric coupling effects and the scaling coefficient $V_0/\hbar\Omega$, the instanton action takes the form of eq 5 of the main text.

Effective-Mode Representation of the Symmetric Coupling

Here we show how and under which conditions the multi-mode effect of the symmetric modes in the nonlocal action can be represented by a single effective mode, which is equivalent to approximating the multi-mode kernel in eq A.2 by the corresponding effective-mode kernel:

$$U_{\mathrm{eff}}(\tau - \tau') \simeq U_{\mathrm{s}}(\tau - \tau');$$
$$U_{\mathrm{s}}(\tau - \tau') = \sum_{i=\mathrm{s}} \tilde{\alpha}_i \exp(-\tilde{\omega}_i|\tau - \tau'|);$$
$$U_{\mathrm{eff}}(\tau - \tau') = U_0 \exp(-\omega_{\mathrm{eff}}|\tau - \tau'|) \tag{A.13}$$

where $U_0 = \sum_{i=\mathrm{s}} \tilde{\alpha}_i$. This is possible only at large $\tilde{B}_{\mathrm{s}}$, when the distribution of the real MD kernel is very narrow. To show this we write each kernel in the following equivalent representation ($X = \tau - \tau'$):

$$U_{\mathrm{s}}(X) \equiv \sum_{i=\mathrm{s}} \tilde{\alpha}_i[1 - \tilde{\omega}_i|X| + {\tilde{\omega}_i}^{2}X^2/2 - \ldots]$$
$$= U_0 - (\tilde{B}_{\mathrm{s}}/2)|X| + \tilde{A}_{\mathrm{s}}X^2/2 - \ldots$$
$$U_{\mathrm{eff}}(X) \equiv U_0[1 - \omega_{\mathrm{eff}}|X| + {\omega_{\mathrm{eff}}}^{2}X^2/2 - \ldots]$$
$$= U_0 - (\tilde{B}_{\mathrm{s}}/2)|X| + ({\tilde{B}_{\mathrm{s}}}^{2}/4U_0)X^2/2 - \ldots \tag{A.14}$$

where $\tilde{A}_{\mathrm{s}} = \sum_{i=\mathrm{s}} \tilde{\gamma}_i^2/4\tilde{\omega}_i$; $\tilde{B}_{\mathrm{s}} = \sum_{i=\mathrm{s}} \tilde{\gamma}_i^2/2\tilde{\omega}_i^2$, and we have introduced the (dimensionless) effective-mode frequency

$$\omega_{\mathrm{eff}} = \tilde{B}_{\mathrm{s}}/2U_0 \equiv \frac{\sum_{i=\mathrm{s}} \tilde{\gamma}_i^{2}/2\tilde{\omega}_i^{2}}{\sum_{i=\mathrm{s}} \tilde{\gamma}_i^{2}/2\tilde{\omega}_i^{3}} \tag{A.15}$$

The expressions on the right-hand side of eq A.14 differ from the quadratic term onward, but this is of little consequence, since the MD kernel falls off rapidly at large $\tilde{B}_{\mathrm{s}}$; as a result, the two kernels differ only in the wings, where the actual kernel is already small for the systems of present interest. This is easily seen from the equation which defines the value of the argument $X = X_0$ where the deviation $\Delta U(X) = U_{\mathrm{s}}(X) - U_{\mathrm{eff}}(X)$ reaches a maximum:

$$\tilde{B}_{\mathrm{s}} \exp(-\omega_{\mathrm{eff}}|X_0| = \sum_{\mathrm{i=s}} (\tilde{\gamma}_i^{2}/2\tilde{\omega}_i^{2}) \exp(-\tilde{\omega}_i|X_0|) \tag{A.16}$$

At large $\tilde{B}_{\mathrm{s}}$, $|X_0|$ is large enough, so that at $X = X_0$ the MD kernel has fallen off significantly from its maximum U_0. For the compounds treated in the present study, $\Delta U(X_0)/U_0$ does not exceed 0.2, as illustrated in Figure 1.

Comparison with AIM

Here we provide a brief summary of the approximations involved in the evaluation of zero-point tunneling splittings by the RIM and by the AIM, which are based on the same Hamiltonian given by eq 1 of the main text but adopt different approximations. For brevity we consider only symmetric coupling, as it has by far the strongest effect, and therefore omit the tilde from the symbols.

In the rainbow approximation the splitting is defined by eqs 3−5 of the main text, in which the pre-exponent is given by eq 4 and the instanton action by eq 5. This action consists of the main part, which is the instanton action of a 1D motion in the adiabatic potential along the reaction coordinate, and a positive correction, which is evaluated without approximation of the memory kernels but with an approximate instanton solution instead.

The AIM, on the other hand, is based on the conventional approach which uses approximations for these kernels. It starts with exact solutions for the instanton action at $T = 0$ for 2D systems, obtained in the adiabatic approximation (AA) and the sudden approximation (SA), which are then combined into a

dx.doi.org/10.1021/jp4073608 | J. Phys. Chem. A XXXX, XXX, XXX−XXX

generalized approximate expression for the instanton action of a MD system. This is done by separating the coupled modes into "fast" modes and "slow" modes relative to the imaginary frequency under the barrier and treating those in the AA and SA, respectively. The fast modes renormalize the 1D motion along the reaction coordinate leading to the effective 1D potential $U_C^{\text{eff}}(x)$ (i.e. a potential that is partially adiabatic) and coordinate-dependent mass $m^{\text{eff}}(x)$. Since at $T = 0$ the energy $E = 0$ is preserved along the instanton path, the instanton action of this effective 1D motion is given by

$$S_I^{1D} = \int_{-\Delta x}^{\Delta x} dx \sqrt{2m^{\text{eff}}(x) U_C^{\text{eff}}(x)} \tag{A.17}$$

The slow modes shorten the tunneling distance and thus enhance tunneling, reflected in corrections δ_s to this action, which reduces it. The "long action" S_I^{1D}, calculated for $E = 0$, is replaced by the "short action", $S_I^{1D}(E_0)$, evaluated for the zero-point level E_0 in $U_C^{\text{eff}}(x)$. This allows simplification of the expression for the pre-exponent of the tunneling splitting (as well as generalization to tunneling splitting of excited levels). The zero-point tunneling splitting assumes the final form

$$\Delta_0 = \frac{\hbar\omega_0}{\pi} \exp\left\{\frac{-S_I^{1D}(E_0)}{1 + \sum'_{i=s}\delta_i}\right\} \tag{A.18}$$

where the sum is restricted to the slow modes. Details, including the modification related to the presence of antisymmetric coupling, can be found in ref 19 and references therein.

AUTHOR INFORMATION

Corresponding Author

*E-mail: zorka.smedarchina@nrc-cnrc.gc.ca.

Notes

The authors declare no competing financial interest.

ACKNOWLEDGMENTS

This work was partially financed by Xunta de Galicia through Grant No. 2012/314.

REFERENCES

(1) Smedarchina, Z.; Siebrand, W.; Fernández-Ramos, A.; Meana-Panēda, R. Mechanisms of Double Proton Transfer. Theory and Applications. *Z. Phys. Chem.* **2008**, *222*, 1291−1303.

(2) Smedarchina, Z.; Siebrand, W.; Fernández-Ramos, A. Multiple Proton Transfer: From Stepwise to Concerted. *Hydrogen-Transfer Reactions*, Hynes, J. T.; Klinman, J. P.; Limbach, H.-H.; Schowen, R. L., Eds.; Wiley-VCH; Weinheim, Germany, 2007; pp 895−945.

(3) Madeja, F.; Havenith, M. High-Resolution Spectroscopy of Carboxylic Acid in the Gas Phase: Observation of Proton Transfer in $(DCOOH)_2$. *J. Chem. Phys.* **2002**, *117*, 7162−7167.

(4) M. Ortlieb, M.; Havenith, M. Proton Transfer in $(HCOOH)_2$: An IR High-Resolution Spectroscopic Study of the Antisymmetric C-O Stretch. *J. Phys. Chem. A* **2007**, *111*, 7355−7363.

(5) Chang, Y. T.; Yamaguchi, Y.; Miller, W. H.; Schaeffer, H. F., III An Analysis of the Infrared and Raman Spectra of the Formic Acid Dimer $(HCOOH)_2$. *J. Am. Chem. Soc.* **1987**, *109*, 7245−7253.

(6) Shida, N.; Barbara, P. F.; Almlöf, J. A Reaction Surface Hamiltonian Treatment of the Double Proton Transfer of Formic Acid Dimer. *J. Chem. Phys.* **1991**, *94*, 3633−3643.

(7) Ushiyama, H.; Takatsuka, K. Successive Mechanism of Double-Proton Transfer in Formic Acid Dimer: A Classical Study. *J. Chem. Phys.* **2001**, *115*, 5903−5912.

(8) Vener, M. V.; Kühn, O.; Bowman, J. M. Vibrational Spectrum of the Formic Acid Dimer in the OH Stretch Region. A Model 3D Study. *Chem. Phys. Lett.* **2001**, *349*, 562−570.

(9) Loerting, T.; Liedl, K. R. Toward Elimination of Discrepancies between Theory and Experiment: Double Proton Transfer in Dimers of Carboxylic Acids. *J. Am. Chem. Soc.* **1998**, *120*, 12595−12600.

(10) Tautermann, C. S.; Voegele, A. F.; Liedl, K. R. The Ground-State Tunneling Splitting of Various Carboxylic Acid Dimers. *J. Chem. Phys.* **2004**, *120*, 631−637.

(11) Luckhaus, D. Concerted Hydrogen Exchange Tunneling in Formic Acid Dimer. *J. Phys. Chem. A* **2005**, *110*, 3151−3158.

(12) Mil'nikov, G. V.; Kühn, O.; Nakamura, H. Ground-State and Vibrationally Assisted Tunneling in the Formic Acid Dimer. *J. Chem. Phys.* **2005**, *123*, 074308-(1−9).

(13) Smedarchina, Z.; Fernández-Ramos, A.; Siebrand, W. Calculation of the Tunneling Splitting in the Zero-Point Level of the CO-Stretch Fundamental of the Formic Acid Dimer. *Chem. Phys. Lett.* **2004**, *395*, 339−345.

(14) Smedarchina, Z.; Fernández-Ramos, A.; Siebrand, W. Tunneling Dynamics of Double Proton Transfer in Formic Acid and Benzoic Acid Dimers. *J. Chem. Phys.* **2005**, *122*, 134309−134312.

(15) Siebrand, W.; Smedarchina, Z.; Zgierski, M. Z.; Fernández-Ramos, A. Proton Tunneling in Polyatomic Molecules: A Direct-Dynamics Instanton Approach. *Int. Rev. Phys. Chem.* **1999**, *18*, 5−41.

(16) Smedarchina, Z.; Fernández-Ramos, A.; Siebrand, W. DOIT: A Program to Calculate Thermal Rate Constants and Mode-Specific Tunneling Splittings Directly from Quantum-Chemical Calculations. *J. Comput. Chem.* **2001**, 22−801.

(17) Remmers, K.; Meerts, W. L.; Ozier, I. Proton Tunneling in the Benzoic Acid Dimer Studied by High Resolution Ultraviolet Spectroscopy. *J. Chem. Phys.* **2000**, *112*, 10890−10895.

(18) Borst, D. R.; Roscoli, J. R.; Pratt, D. W.; Florio, G. M.; Zwier, T. S.; Müller, A.; Leutwyler, S. Hydrogen Bonding and Tunneling in the 2-Pyridone·2-Hydroxypyridine Dimer. Effect of Electronic Excitation. *Chem. Phys.* **2002**, *283*, 341−354.

(19) Smedarchina, Z.; Siebrand, W.; Fernández-Ramos, A.; Marínez-Núñez, E. New Interpretation of Ground- and Excited-State Tunneling Splitting in 2-Pyridone·2-Hydroxypyridine. *Chem. Phys. Lett.* **2004**, *386*, 396−402.

(20) Roscoli, J. R.; Pratt, D. W.; Smedarchina, Z.; Siebrand, W.; Fernández-Ramos, A. Proton Transfer Dynamics via High Resolution Spectroscopy in the Gas Phase and Instanton Calculations. *J. Chem. Phys.* **2004**, *120*, 11351−11354.

(21) Smedarchina, Z.; Siebrand, W.; Fernández-Ramos, A. The Rainbow Instanton Method: A New Approach to Tunneling Splitting in Polyatomics. *J. Chem. Phys.* **2012**, *137*, 224105−224116.

(22) Tautermann, C. S.; Voegele, A. F.; Loerting, T.; Liedl, K. R. An Accurate Semiclassical Method to Predict Ground-State Tunneling Splittings. *J. Chem. Phys.* **2002**, *117*, 1962−1966.

(23) Meana-Pañeda, R.; Truhlar, D. G.; Fernández-Ramos, A. Least-Action Tunneling Transmission Coefficient for Polyatomic Reactions. *J. Chem. Theory Comput.* **2010**, *6*, 6−17.

(24) Mil'nikov, G. V.; Nakamura, H. Practical Implementation of the Instanton Theory for the Ground-State Tunneling Splitting. *J. Chem. Phys.* **2001**, *115*, 6881−6897.

(25) Richardson, J. O.; Althorpe, S. C.; Wales, D. J. Ring-Polymer Instanton Method for Calculating Tunneling Splittings. *J. Chem. Phys.* **2011**, *134*, 054109−054119.

(26) Richardson, J. O.; Althorpe, S. C.; Wales, D. J. Instanton Calculations of Tunneling Splittings for Water Dimer and Trimer. *J. Chem. Phys.* **2011**, *135*, 124109−124120.

(27) Rommel, J. B.; Kästner, J. Adaptive Integration Grids in Instanton Theory Improve the Numerical Accuracy at Low Temperature. *J. Chem. Phys.* **2011**, *134*, 184107−184116.

(28) Ueda, K.; Oguni, M. Quantum Tunneling in the Quadruple Proton Rearrangement of a Hydroxyl Hydrogen-Bond Ring in Calix[4]arene. *J. Phys. Chem. B* **2012**, *116*, 14470−14476.

(29) Smedarchina, Z.; Fernández-Ramos, A. RIM, a Code for Calculating Zero-Point Level Splittings by the Rainbow Instanton Method. *Available upon request*.
(30) Smedarchina, Z.; Siebrand, W.; Zgierski, M. Z.; Zerbetto, F. Dynamics of Molecular Inversion: An Instanton Approach. *J. Chem. Phys.* **1995**, *102*, 7024−7034.
(31) Siebrand, W.; Smedarchina, Z.; Fernández-Ramos, A. Communication: Selection Rules for Tunneling Splitting of Vibrationally Excited Levels. *J. Chem. Phys.* **2013**, *139*, 021101−021104.
(32) Lüttschwager, N. O. B.; Wassermann, T. N.; Coissan, S.; Suhm, M. A. Vibrational Tuning of the Hydrogen Transfer in Malonaldehyde—a Combined FTIR and Raman Study. *Mol. Phys.* **2013**, *14*−*15*, 2211−2227.
(33) Siebrand, W.; Smedarchina, Z.; Fernández-Ramos, A. Tunneling Splitting and Level Ordering in a CO-Stretch Fundamental of the Formic Acid Dimer. *Chem. Phys. Lett.* **2008**, *459*, 22−26.
(34) Oppenländer, A.; Rambaud, C.; Trommsdorff, H. P.; Vial, J.-C. Translational Tunneling of Protons in Benzoic Acid Crystals. *Phys. Rev. Lett.* **1989**, *63*, 1432−1435.
(35) Rambaud, C.; Trommsdorff, H. P. Cooperative Proton Transfer and Tunneling in Dye Doped Benzoic Acid Crystals. *Chem. Phys. Lett.* **1999**, *306*, 124−132.
(36) Brougham, F. B.; R. Caciuffo, R.; Horsewill, R. Coordinated Proton Transfer in a Cyclic Network of Four Hydrogen Bonds in the Solid State. *Nature* **1999**, *397*, 241−243.
(37) Fernández-Ramos, A.; Smedarchina, Z.; Pichierri, F. Proton Tunneling in Calix[4]arenes; A Theoretical Investigation. *Chem. Phys. Lett.* **2001**, *343*, 627−632.
(38) Vener, M. V.; Sauer, J. Vibrational Spectra of the Methanol Tetramer in the OH-Stretch Region. Two Cyclic Isomers and Concerted Proton Transfer. *J. Chem. Phys.* **2001**, *114*, 2623−2628.